



# Do EnChroma glasses improve performance on clinical tests for red-green color deficiencies?

CAT PATTIE,<sup>1,\*</sup>  STACEY ASTON,<sup>2</sup> AND GABRIELE JORDAN<sup>1</sup>

<sup>1</sup>*Biosciences Institute, Newcastle University, United Kingdom*

<sup>2</sup>*Department of Psychology, Durham University, United Kingdom*

\**c.e.pattie1@ncl.ac.uk*

**Abstract:** We investigated the claims of EnChroma that their notch filters aid chromatic discrimination in color-vision deficiencies (CVD). Few research studies have addressed these claims and reports are still inconclusive, mainly due to small sample sizes. We here add to previous research finding little evidence to support the benefits of EnChroma lenses. Comparing the performance of 86 well-categorized CVD observers and 24 controls on two clinical tests we report no overall improvement when EnChroma lenses were worn. In line with previous studies, our results imply an improvement in discrimination for some colors while worsening discrimination for others. A model was constructed computing discrimination changes for different groups of ideal observers corroborating our behavioral outcomes. Taken together, our results do not support the use of EnChroma notch filters for the improvement of color discrimination in CVD.

© 2022 Optica Publishing Group under the terms of the [Optica Open Access Publishing Agreement](#)

## 1. Introduction

In a world with an ever-growing demand for processing information based on color, individuals with color-vision deficiencies (CVD) may have a real disadvantage. Normal human observers typically have three types of retinal cone photopigments sensitive to long- (L), middle- (M), and short wavelengths (S) respectively, but 8% of men (0.4% of women) suffer from an X-Chromosome linked form of red-green color deficiency (equating to 2.64 million affected people in the UK alone). The severity and subtype of red-green CVD depends on whether the L or M cones are absent (2% males), or spectrally shifted (6% males). Furthermore, the color vision of anomalous trichromats can vary from very mild, and almost indistinguishable from normal, to very severe depending on the spectral separation of the two middle- to long-wave photopigment variants [1]. For a review on the underlying molecular genetics of CVD please see Neitz and Neitz [2].

The everyday challenges of affected individuals have been summarized by Cole [3]. They range from difficulties discriminating between surface colors or lights, segmenting objects from backgrounds, naming colors accurately, to failing or slowing in tasks involving visual search. Consequently, there are restrictions to CVD individuals by professional bodies where color quality (e.g. manufacturing) or health and safety linked to color signaling (e.g. public transport) are paramount.

However, although congenital color-vision deficiencies are not a protected characteristic, equal opportunity laws (e.g. UK Equality Act 2010) demand that employers demonstrate that they are not unlawfully discriminating against color-deficient recruits and should, where possible, put reasonable adjustments in place to allow affected persons to compensate for their deficiency. In this context, the promise of commercially available visual aids to improve the color discrimination of CVD individuals (e.g. EnChroma [4]) has increased the public interest in such aids. Perhaps not surprisingly it has also triggered an increase in research since evidence for the effectiveness of such glasses is still relatively sparse.

The use of spectacles or filters to create interocular differences to help those with CVD goes back to Seebeck [5] and has been summarized by Sharpe and Jägle [6]. A more comprehensive review of a larger variety of ophthalmic devices to manage or aid CVD has been provided by Salih et al. [7]. However, despite the promise of commercial companies to improve the color discrimination of CVD individuals, results are mixed. An excellent attempt to model the efficacy of a large variety of lenses to help anomalous trichromats discern Munsell surfaces with known reflectance spectra, including the D-15, has been offered by Moreland et al. [8]. They used 43 commercial filters from five manufacturers and calculated the ratio of standard deviations of the filtered to unfiltered chromaticities (to provide an enhancement factor;  $E$ ) for a standardized, equiluminant protanomalous (Pa) and deuteranomalous (Da) visual system, respectively. In addition, guided by the European Standard agency [9], they also calculated the visual attenuation quotient for three saturated stimuli representing red, yellow and green traffic lights. Moreland and colleagues report a spread of  $E$  values for both axes of their modelled Pa and Da cone contrast space with most filters demonstrating a compression rather than expansion of perceivable chromaticities. None of the filters achieved the desired threshold value of  $E$  to be useful in ecological settings and, concerningly, most of the filters did not meet the signal detection standard for traffic lights and were therefore deemed unsafe. Subsequently, Moreland et al. [10] compared Farnsworth-Munsell 100-Hue (FM100 Hue) test Total Error Scores of one protanomalous and one deuteranomalous observer with and without prescribed ColorView aids and modelled the difference in chromaticities of the FM100 Hue caps with and without the aids. They found that the Total Error Score of their observers increased with ColorView, and this was also reflected by their model; ColorView increased chromatic scatter, disrupted chromatic ordering and caused a shift across the deuteranomalous and protanomalous chromaticity diagrams.

We here focus on the evaluation of lenses produced by EnChroma, one of the current market leaders, who designed notch filters that block the transmittance of light in the overlapping regions of L- and M cone absorptions aiming to increase the spectral separation between signals. As a consequence, color contrast should be optically enhanced in some parts of the spectrum providing a more salient signal to some wearers. The company's marketing strategy is very successful, though the efficacy of their lenses seems to contrast somewhat with the many testimonials of color-deficient individuals claiming that they can 'see colors for the first time'.

Research on EnChroma lenses has been relatively sparse, mostly reporting no support for the initial claims made by the company to 'cure color blindness' or 'seeing new colors' [11–14]. More specifically, EnChroma glasses were tested on participants with known color deficiencies and tests comprising a variety of clinical diagnostic tools for red-green color vision including the CAD, Pseudoisochromatic Plate Tests and FM100 Hue test or D-15 [13–15], or digital versions of the Ishihara Plates and FM100 Hue test [12]. None of the studies reported a clear, overall improvement for CVD participants in the performance on the clinical tests, although Varikuti et al [15] found a reduced error score on the Ishihara Plates in half of their small sample of deuteranomalous participants, and a reduced confusion index on the D-15 in a very small sample of protanomalous participants. Two studies reported a change in subjective color perception.

A recent paper by Werner and colleagues [16] provided evidence for an increase in L-M contrast vision in CVD participants after prolonged wearing of EnChroma glasses. Rather than using standardized tests for color deficiencies, they modulated the red-green contrast of small Gabor patches along the L-M axis and luminance axis of DKL color space [17] and asked a small number of anomalous trichromats of known type and two normal controls which of two test patches in a triplet of patches displayed on a monitor was most similar to a standard patch. Intriguingly, the scaled response functions of their anomalous observers improved after 11 days of wearing the glasses. A similar finding after prolonged use of the filters, measuring cone contrast and color naming, has just been confirmed by Rabin and colleagues [18]. Interestingly,

they also report a change in cone-specific VEPs in a subset of CVD participants suggesting that some neural compensation takes place after prolonged adaptation to the notch filters.

Here, we report the results of a study conducted in 2017 and 2018 using a varied sample of well-classified CVD participants, which is larger than samples utilized in previous studies. Although conducted independently, it expands on a study by Gómez-Robledo et al [13] and confirms their results of a rotation in FM confusion axes with increased discrimination in some areas of color space but losses in other parts. We did not see an overall improvement in color discrimination. In addition to our behavioral data, we provide an ideal-observer-type model predicting EnChroma induced changes in performance of different observer types on the FM100 Hue test.

## 2. Materials and methods

### 2.1. Behavioral study

#### 2.1.1. Participants

118 observers (22 females) (mean age in years = 34.03, SD = 16.71) were recruited using a variety of channels including newspaper articles, posters, social media posts, public talks and University recruitment platforms. Of those 118 volunteers, 86 were color deficient, 24 were normal trichromats, and eight participants were excluded as their color-vision type could not be specified. Table 1 shows the breakdown of CVD subtypes and mean ages in our sample. The Faculty of Medical Sciences ethics board at Newcastle University approved the study (1475/3905). All observers provided written informed consent prior to taking part in the study. Observers took part in the study between July 2017 and June 2018.

**Table 1. Number, mean age and mean Medmont C-100 settings, Rayleigh match (RM) midpoint and range of seven subgroups of color vision; normal, deuteranomalous (Da), extreme deuteranomalous (eDa), deuteranope (D), protanomalous (Pa), extreme protanomalous (ePa), and protanope (P)**

	Normal	Deutan deficiency			Protan deficiency		
		Da	eDa	D	Pa	ePa	P
n	24	30	10	9	12	5	20
Age (yrs)	21.21	34.50	27.80	45.44	36.83	48.80	43.40
Mean Medmont setting	-0.917	1.587	1.800	1.711	-2.933	-2.980	-2.930
Mean RM midpoint	45.652	16.581	25.420	n.a.	58.904	41.400	n.a.
Mean RM range	2.548	5.1000	17.969	n.a.	5.058	54.440	n.a.

#### 2.1.2. Color vision categorization

Observers were categorized as normal (N), deuteranomalous (Da), extreme deuteranomalous (eDa), deuteranope (D), protanomalous (Pa), extreme protanomalous (ePa), and protanope (P) using two standardized tests of color vision: Oculus anomaloscope and Medmont C-100.

The Oculus anomaloscope uses the Rayleigh equation and is widely considered as the gold standard in classifying both the type and severity of color deficiencies. Observers view a 2-deg bipartite circular field with their dominant eye and adjust the ratio of a red (666 nm) and green (549 nm) light mixture to match a monochromatic standard yellow light (589 nm). The brightness of the yellow standard is adjustable and differs markedly between deutan and protan individuals. The Rayleigh matching range is the range of all red/green ratios accepted as a perfect match and provides an indication of the individual's color discrimination ability. Midpoints typically fall into discrete categories and are used to classify an individual's type of CVD. Observers made Rayleigh Matches in a dark room. See Figure S1 in supplementary materials for Rayleigh match

mid-points and ranges for all observers but dichromats, who cannot discriminate between the red and green spectral lights and make matches for all ratios.

Categorization into protan or deutan subtypes was confirmed using the Medmont C-100, a small, hand-held device requiring observers to minimize the flicker of two LED lights (569- and 626 nm) mixed in a Perspex rod and modulated in counterphase at 16 Hz. The point at which the flicker appears minimal is indicated using a scale from -5 to +5. Settings of less than -2 or more than +2 indicate a protan or deutan classification respectively [19]. Observers adjusted the flicker of the Medmont C-100 five times to produce an average setting. As the Medmont C-100 and the anomaloscope provide different information (estimates of L:M cone ratio and cone spectral sensitivity, respectively), both tests were used to guide CVD classification for each observer or categorize them as normal (see Table 1).

### 2.1.3. Behavioral evaluation of EnChroma glasses

After categorization of observers into CVD subtypes, the FM100 Hue test and the Ishihara Plates (38<sup>th</sup> edition, 2009) were used to determine the effects of the EnChroma lenses (C-25, 58 mm, see Fig. 1(B)) on chromatic discrimination. Tests were performed in a repeated measures design, once without the glasses to establish baseline performance, and a second time after a 30-min adaptation period. The order of the two conditions was not randomized for practical reasons as it would have significantly prolonged the time commitment of our observers. Tests were performed under natural daylight in the open space next to a large glass front and was supplemented by an artificial daylight source, as well as fluorescent ceiling lighting that could not be turned off. During each testing session, sky conditions were recorded as clear blue, some clouds, or overcast. A sample of typical light levels were measured using a Konica Minolta Illuminance Spectrophotometer CL-500A. These light levels ranged from 1073-1926 lux.

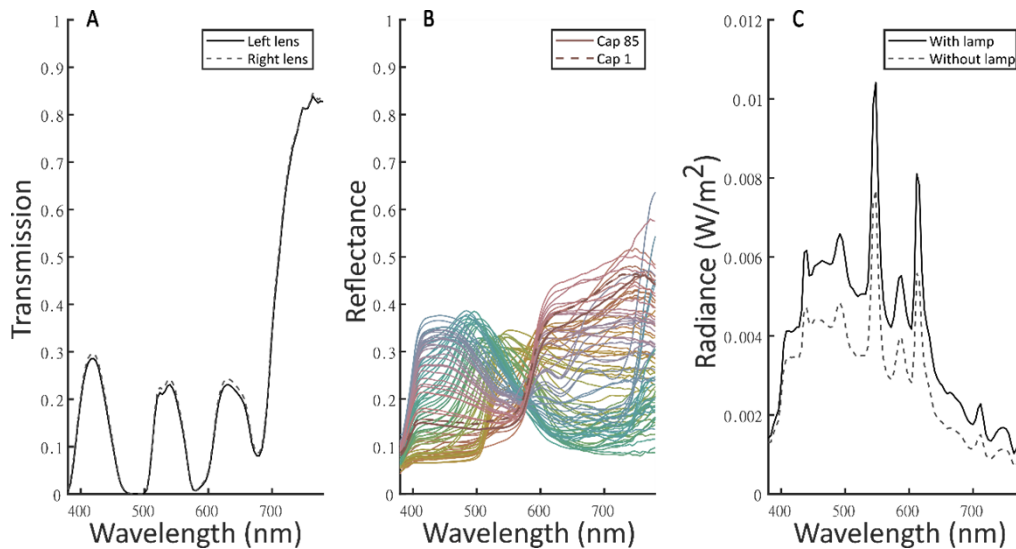


**Fig. 1.** Spectral Measurements. A. The transmission spectra of the EnChroma glasses for both the left and right lens. B. The reflectance spectra of the 85 caps in the FM100 Hue test, where line color corresponds to the color of the cap. C. The incident illumination during testing with and without the D65 lamp switched on.

Observers were asked to read the first 25 plates of the Ishihara Plate test and error score were recorded as the number of plates read incorrectly. To complete the FM100 Hue test, observers were told they had approximately two minutes to complete each of the four boxes. They were

given one box at a time, in no particular order, and were instructed to arrange the caps according to the closest hue from one cap to the next. The arrangement of caps was used to calculate a total error score (TES), confusion angle (CA), confusion index (CI) and selectivity index (SI) as per Vingrys and King-Smith [20]. For more information see 2.24 Data Analyses.

Observers were then given the EnChroma lenses and wore them for a 30-min adaptation period, during which they completed a demographics questionnaire and chatted to the experimenter. Following the adaptation period, and with the EnChroma glasses on, observers completed the FM100 Hue test again and then the Ishihara Plates in reverse order to avoid the effects of memorizing the digits.

#### 2.1.4. Data analyses

We compared the performance measures on each test between baseline (without glasses) and test condition (with glasses). The FM100 Hue measures were calculated as follows. The total error score (TES) is the score of the joined cap arrangement for all boxes: an error score is calculated for each cap as the sum of the differences between the cap's value and the adjacent cap's values minus two. The TES is the sum of each cap's error score. The confusion angle (CA), confusion index (CI), and selectivity index (SI) were calculated according to Vingrys and King-Smith's Moment of Inertia method. Briefly, CA defines the axis in CIELUV along which color discrimination is poorest [20]. CI is a measure of how much poorer discrimination along the axis is compared to the ideal observer; and SI is a measure of the relative discrimination ability between the poorest and best axis. These measures use the tristimulus values of each cap viewed under a standard illumination (Illuminant C) transformed to CIELUV perceptually uniform color space. Since our observers did not perform the FM100 Hue test under Illuminant C, we computed the caps' CIELUV values using our own spectral measurements (see 2.2 Spectral Measurements).

## 2.2. Spectral measurements

Spectral measurements were taken with a PR650 SpectraScan spectroradiometer (Photo Research, Syracuse, USA). To measure the spectral reflectance of the FM100 Hue caps we first measured the light spectra reflected from each cap placed under a lamp fitted with a D65 bulb. We also measured the light reflected from a white reflectance standard (Ocean Optics WS-1 Diffuse Reflectance Standard) to recover the reflectance of each cap (Fig. 1(A)) by pointwise division.

The transmission spectra of the EnChroma glasses were measured for each lens separately and are shown in Fig. 1(B). We recovered the transmission of each lens by performing a pointwise division of the spectral measurements reflected from the white reflectance standard with and without the filters under D65.

As observers completed the FM100 Hue test in conditions of natural daylight, we also used the white reflectance standard to obtain a daylight measurement in the experimental area. The spectral power distribution of the illumination was taken as the light reflected from the reflectance standard when placed in the same position as the FM100 Hue caps during the task. Measurements were taken with and without the D65 lamp turned on (see Fig. 1(C)) on 1<sup>st</sup> Aug 2019 and are the mean of three successive captures.

Measurements from the PR650 SpectraScan have a wavelength resolution of 4 nm in the range 380-780 nm. For the purposes of our calculation, we interpolated the measured spectra for the range 400-700 nm in 1 nm steps.

## 2.3. Modelling

### 2.3.1. Modelling Overview

In addition to collecting behavioral data, we also undertook a modelling exercise to further explore how beneficial the EnChroma lenses would be in a situation where the wearer could



optimally exploit the signals available to them at the retina (regardless of observer type), and thus, optimally represented the changed signals available at the retina when wearing the EnChroma glasses. To do this, we first defined what we refer to as an “optimal color space” for each observer type. As explained below, these were defined such that they optimally represented differences in retinal signals produced by a set of Munsell surface reflectances simulated to appear under the daylight illumination present during the behavioral experiment. By including a von Kries transformation as part of the process that maps reflected spectra to a point in optimal color space, this also allowed for adaptation to the EnChroma filters, so that reflected light as experienced through the lenses could also be mapped to a point in optimal color space. We used these spaces to create a measure of overall change in discriminability when the EnChroma lenses are worn and to simulate an observer completing the FM100 Hue test. To simulate responses of an ideal observer to the FM100 Hue test, we arranged the caps in optimal color space using a Travelling Salesman algorithm.

### 2.3.2. Optimal color spaces

For each observer type, we derived an optimal color space in which we are able to quantify the changes in discriminability for an ideal observer who optimally exploits the information available from the cone responses. The spaces were derived by performing principal component analysis (PCA) on sets of cone responses, inspired by Ruderman et al. [21], after scaling the cone responses using a von Kries transformation [22]. We believe that the color spaces created in this way are optimal as PCA finds the axes of maximum variation in the data. Ruderman et al. originally performed PCA on a set of L, M, and S values obtained from hyperspectral images of natural scenes and found that the principal axes of variation (the components) were a luminance axis ( $L + M + S$ ) and two chromatic axes ( $L - M$  and  $S - (L + M)$ ), suggesting that the color channels identified early in the visual system from electrophysiological recordings have evolved to optimally trade-off the cone responses for maximum discrimination [17,23]. Our derivation of optimal color spaces is based on the assumption that the post-receptoral color channels may be able to adapt in color-deficient observers to optimally represent the available information from the remaining and/or anomalous cone types.

To derive the optimal color spaces for each subtype of observer, we first modelled the light reaching the eye from the subset of matte Munsell surface reflectances under the daylight spectrum that we measured (Fig. 1(A)) without the EnChroma filter by performing pointwise multiplication of the reflectances and illumination spectrum (when we add in the EnChroma filter later we perform pointwise multiplication of the reflectances, the illumination spectrum, and the EnChroma transmission spectrum). Secondly, we used the DeMarco cone fundamentals [24] to compute a set of cone responses ( $L$ ,  $M$ ,  $S$ ,  $L'$ , and  $M'$ ) for each patch (pointwise multiplication of the reflected light with the cone sensitivity curves). The cone responses were scaled by assuming perfect knowledge of the cone values of the daylight illumination ( $L_I$ ,  $M_I$ , and  $S_I$  for a normal trichromat but different sets of cone values for other observer types) and scaling by these values within each cone class (all  $L$  values become  $L/L_I$  and so on; a von Kries transformation to add an element of color constancy to our model). We then created the optimal color spaces for each observer type by performing PCA on the corresponding von Kries-scaled cone responses for all Munsell surfaces. The components produced by the PCA are the axes of the optimal color spaces. The recovered coefficients used to transform stimulus values from cone space to optimal color space for each observer type are given in Table 2, where we also name each axis. For normal trichromats and anomalous trichromats, optimal color space is three dimensional and, as can be seen from the coefficients in Table 2, one of the axes is always a luminance axis and the other two are chromatic axes. For dichromats, optimal color space is two dimensional with a luminance axis and one chromatic axis. To express any other surface in this color space we compute the appropriate cone responses (dependent on observer type), von Kries scale these responses by an

estimate of the incident illumination, then transform the cone responses to optimal color space using the appropriate set of coefficients (for the observer type).

**Table 2. Coefficients for transforming von Kries scaled cone responses to optimal color space for each observer type**

Observer Type	Coefficients			Axis Name
	Cone 1	Cone 2	Cone 3	
Normal Trichromat	0.61	0.61	0.51	Lum
(Cones 1-3 are L, M, S)	-0.43	-0.28	0.86	S-(L + M)
	-0.67	0.74	-0.09	L-M
Deuteranomalous	0.61	0.61	0.50	Lum
(Cones 1-3 are L, L', S)	-0.37	-0.34	0.87	S-(L + M)
	-0.70	0.71	-0.02	L-M
Protanomalous	0.61	0.61	0.51	Lum
(Cones 1-3 are M', M, S)	-0.39	-0.33	0.86	S-(L + M)
	-0.69	0.72	-0.04	L-M
Deuteranope	0.74	0.67	N/A	Lum
(Cones 1-2 are L, S)	-0.67	0.74	N/A	S-L
Protanope	0.73	0.68	N/A	Lum
(Cones 1-2 are M, S)	-0.68	0.73	N/A	S-M

Note that while the changes in the coefficients are small for each observer type, only small changes in the coefficients are needed for large changes in behavior. This will become evident later when we see how much model predictions vary for the different observer types despite the small changes in coefficients (see sections 3.3.1 and 3.3.2).

### 2.3.3. Ideal observer models

We created an ideal observer for each type of CVD that arranges the FM100 caps within each optimal color space respectively. The goal of the observer in the FM100 Hue test is to order the caps in such a way that the total color differences between adjacent caps are minimized. We formalized this task to be the minimization of the sum of the Euclidian distances in optimal color space between adjacent caps. This is equivalent to solving the Travelling Salesman Problem (TSP). We adopted a solver-based approach to solving the TSP in MATLAB following the steps detailed at <https://uk.mathworks.com/help/optim/ug/travelling-salesman-problem.html> (code available online, see Supplemental Materials). As the FM100 Hue test is completed box by box with the end caps fixed, we also enforced this upon our ideal observer. We complete the travelling salesman problem for each box, adding the constraint that the two end caps must be next to each other in the solution (by setting that distance to zero so that it appears in the solution). Since the observer is expected to arrange the caps based on color appearance, we ignored the luminance axes for normal and anomalous trichromat observers, choosing to have our ideal observer arrange the caps in the chromaticity plane (defined by the L-M and S-(L + M) axes) of optimal color space. However, for dichromatic observers, we arrange the caps in the plane defined by both their chromatic axis and luminance axis, as while the FM100 Hue caps are designed to be equiluminant for trichromat observers, this will not be preserved in dichromats and could result in an extra cue for discrimination.

### 2.3.4. Open practice statement

The surface reflectance functions for each FM100 Hue test cap (measured in-house), the transmission spectra of the outdoor EnChroma glasses (measured in-house), the MATLAB code

for the ideal observer analysis and for scoring the FM100 Hue test, and all analysis scripts are available online at <https://osf.io/at598/>.

### 3. Results and discussion

#### 3.1. Behavioral measures

##### 3.1.1. Ishihara plates

No significant differences were found between Ishihara error scores at baseline and EnChroma condition for eDa, D, Pa, ePa or P. However, the mean error score of normal observers significantly decreased from 1.041 at baseline to 0.500 with EnChroma ( $t(23) = 2.72, p = .012$ ) and the mean error score of deuteranomalous observers decreased from a mean of 18.27 at baseline to 17.27 with EnChroma ( $t(29) = 2.57, p = .016$ ). See Table 3 and Fig. 2 for a full report of the results.

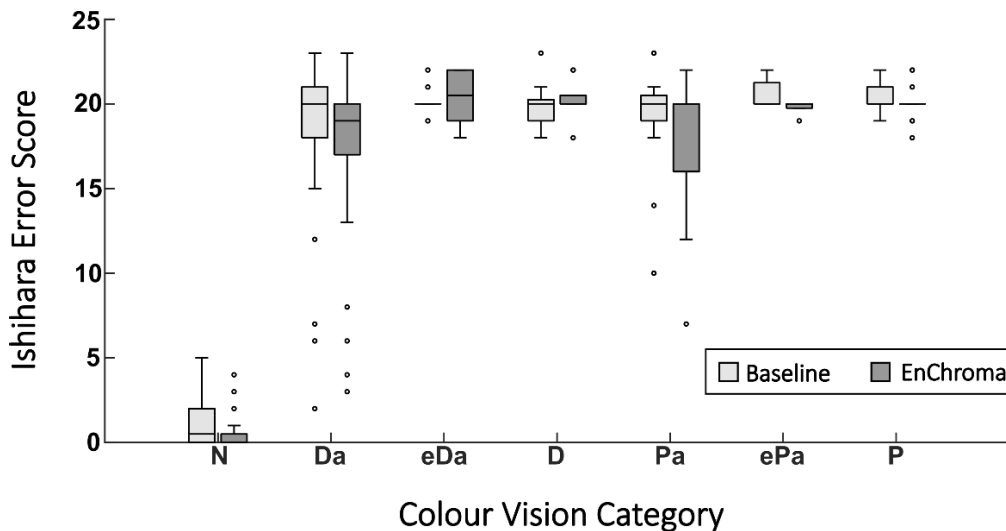


**Fig. 2.** Boxplot showing error scores on Ishihara Plates for seven color-vision categories. For abbreviations and number of observers, see Table 1. Light bars indicate error scores for the baseline condition, dark bars show errors for the EnChroma condition.

**Table 3.** Mean and standard deviations of Ishihara errors for each group of observers and t-test results for the baseline versus EnChroma conditions

	Baseline		EnChroma		t-test
	Mean	SD	Mean	SD	t (p)
Normal	1.04	1.40	0.50	1.06	2.72 (0.012)
Da	18.27	5.05	17.27	5.25	2.57 (0.016)
eDa	20.20	0.79	20.50	1.51	-0.67 (0.50)
D	20.00	1.41	20.22	1.20	-0.48 (0.645)
Pa	18.92	3.53	17.83	4.49	1.62 (0.133)
ePa	20.60	0.89	19.80	0.45	1.37 (0.242)
P	20.30	0.80	20.05	0.89	1.04 (0.309)

In absolute terms the decrease in Ishihara Plate errors for both normal and deuteranomalous observers was very small (just one error) and will not have caused a change in group membership in Da observers. The change may have been caused by a practice effect, but this would also have



applied to other CVD groups, or by the introduction of luminance cues by the lenses, similar to Mastey et al.'s [11] improvement of O2Amp glasses on CAD performance of deutan observers. Thus, despite there being a statistically significant reduction of errors, it does not translate to a real-world improvement as the mean performance remains considerably poorer than normal. Our results are consistent with those of Gómez-Robledo et al. [13] and Almutairi et al. [12] who report no difference in Ishihara error score with and without EnChroma lenses in place.

### 3.1.2. FM100 hue test

We conducted an in-depth analysis of FM100 Hue performance by not only calculating the total error score (TES), but also calculating the confusion angle (CA), confusion index (CI) and scatter index (SI). Details of all comparisons can be seen in Table 4 and Fig. 3.

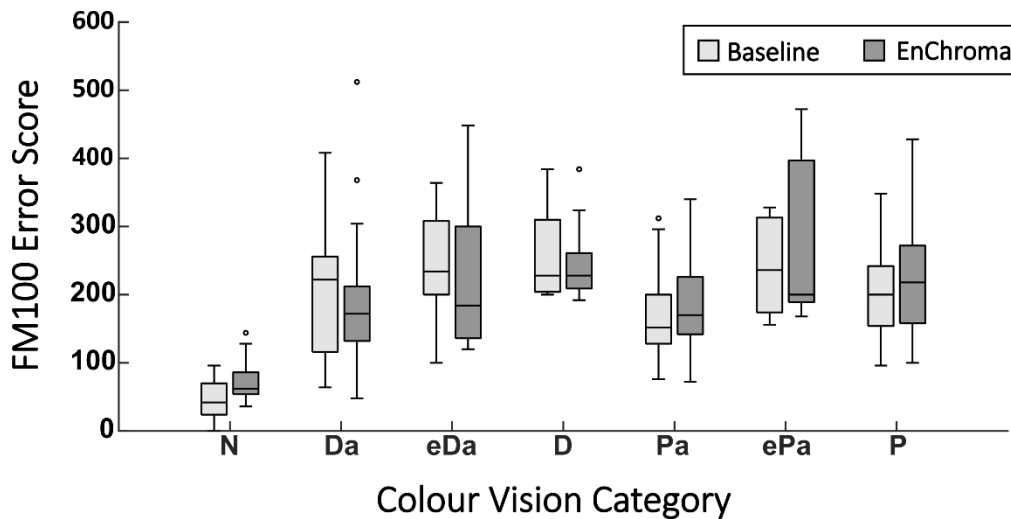


**Fig. 3.** Boxplot showing error scores on FM100 Hue test for seven color-vision categories. For abbreviations and number of observers, see Table 1. Light bars indicate error scores for the baseline condition, dark bars show errors for the EnChroma condition.

No significant differences were found between TES at baseline and with EnChroma for any CVD subtype. However, for normal trichromats TES was significantly higher with EnChroma glasses than at baseline (increase of 26.17 errors,  $t(23) = -4.52$ ,  $p < .001$ ).

As the profile of CA, CI, and SI scores is more informative regarding the changes in color discrimination from baseline to EnChroma condition, they are discussed for each group of observers in the following sections. Results are summarized in Tables 4 to 7.

In normal trichromats, there was no change in CA, but both CI and SI increased significantly in the EnChroma condition. This means that errors became more concentrated in one area and the maximum radius of errors increased compared to that of a perfect arrangement, but the axis along which discrimination is poorest remained the same. Taken together, these results suggest that color discrimination is decreased by EnChroma lenses in those with normal color vision.

In deuteranomalous observers, CA and SI did not change but CI decreased significantly. These results suggest that EnChroma lenses improve discrimination for Da observers, but only along the axis of poorest discrimination.

In protanomalous observers, CA and CI did not change but SI increased significantly. These results suggest that EnChroma lenses improve discrimination in Pa observers, but only along the axis where discrimination was best to begin with.

**Table 4. Means and standard deviations for FM100 Hue Total Error Scores (TES) for each group of observers and t-test results for the baseline versus EnChroma conditions**

	TES				
	Baseline		Test		T-test
	M	SD	M	SD	t <i>p</i>
N	46.50	27.25	72.67	28.81	-4.52 <0.001
Da	204.80	85.56	186.80	91.21	1.76 0.089
eDa	241.60	83.12	217.60	104.85	1.45 0.180
D	256.00	64.78	249.33	63.25	0.49 0.635
Pa	174.00	71.48	184.33	75.02	-1.24 0.242
ePa	241.60	75.87	281.60	133.52	-1.30 0.264
P	202.40	65.39	221.40	76.48	-1.24 0.230

**Table 5. Means and standard deviations for FM100 Hue Confusion Angle (CA) for each group of observers and t-test results for the baseline versus EnChroma conditions**

	CA				
	Baseline		Test		T-test
	M	SD	M	SD	t <i>p</i>
N	-22.05	49.69	1.06	47.74	-1.76 0.091
Da	-10.55	30.68	-7.35	31.74	-0.46 0.647
eDa	-20.70	5.10	0.41	17.84	-3.59 0.006
D	-22.09	5.98	1.10	10.27	-7.00 <0.001
Pa	1.83	33.00	13.09	25.77	-1.35 0.205
ePa	9.67	6.46	24.76	3.09	-4.56 0.010
P	-0.38	8.18	13.12	23.77	-2.48 0.023

**Table 6. Means and standard deviations for FM100 Hue Confusion Index (CI) for each group of observers and t-test results for the baseline versus EnChroma conditions**

	CI				T-test
	Baseline		Test		
	M	SD	M	SD	t p
N	1.27	0.20	1.56	0.28	-5.48 <0.001
Da	2.43	0.74	2.22	0.64	2.75 0.010
eDa	3.04	0.58	2.53	0.73	3.85 0.004
D	3.19	0.48	2.68	0.41	3.33 0.010
Pa	2.14	0.45	2.28	0.45	-1.74 0.110
ePa	2.65	0.40	2.92	0.67	-1.67 0.171
P	2.50	0.47	2.54	0.48	-0.38 0.710

**Table 7. Means and standard deviations for FM100 Hue Selectivity Index (SI) for each group of observers and t-test results for the baseline versus EnChroma conditions**

	SI				T-test
	Baseline		Test		
	M	SD	M	SD	t p
N	1.31	0.18	1.56	0.21	-5.06 <0.001
Da	1.54	0.32	1.48	0.19	1.09 0.286
eDa	1.95	0.23	1.55	0.19	4.60 0.001
D	2.03	0.20	1.57	0.15	6.15 <0.001
Pa	1.45	0.19	1.65	0.20	-3.47 0.110
ePa	1.54	0.15	1.78	0.24	-4.69 0.009
P	1.64	0.18	1.68	0.17	-0.78 0.444

In extreme deuteranomalous observers, there was a significant increase in CA (baseline = -20.70, EnChroma = 0.41) and a significant decrease in CI and SI. Taken together, these results suggest that discrimination was improved overall, but with the axis of worst discrimination rotated.

In extreme protanomalous observers, there was a significant increase in CA (baseline = 9.67, EnChroma = 24.76) and a significant increase in SI but no change in CI. This suggests that EnChroma lenses improve discrimination in ePa observers but only along the axis where their discrimination was already best.

In deuteranopes, there was a significant change in CA and a significant decrease in CI and SI. As for extreme deuteranomalous observers, these results suggest that discrimination was improved overall, but with the axis of worst discrimination rotated.

In protanopes, there was a significant change in CA but no change in CI or SI. Taken together, the results suggest that the lenses do not change overall discrimination ability for P observers but rotate the axis of worst discrimination.

Thus, in general, EnChroma had no effect on the total error scores (TES) of CVD individuals in arranging the caps in the hue circle and the significant reduction in discrimination scores for normal controls was likely a reflection of the significant increase in their SI and CI scores.

The CA, CI and SI profiles in CVD observers suggest that the impact of EnChroma on chromatic discrimination is complex and different depending on CVD subtype. Most notably, despite no change in TES for deuteranomalous and extreme deuteranomalous observers, the decrease in CI (as well as a change in CA and decrease in SI for extreme deuteranomalous observers) suggest that EnChroma lenses may improve discrimination in some areas, without resulting in a total improvement in discrimination ability. Thus, there may be discrimination gains between some hues, but losses between others.

Our results are in line with those of Almutairi et al. [12] and Gómez-Robledo et al. [13] who found no change in overall discrimination, but an increase in SI, suggesting that EnChroma lenses increase the randomness of errors in the FM100 Hue test. However, they did not find a significant change in either CA or CI for any of their groups, whereas some significant changes were found in the present study. This could be due to our much larger sample size, allowing for more robust comparisons within groups.

On the other hand, there is some research suggesting an improvement on clinical color vision tests as a result of EnChroma. Varikuti et al. [15] reviewed performance of 19 patients who had completed Ishihara Plates and Farnsworth D-15 without and with EnChroma, analysing the data from each eye independently. EnChroma were found to reduce Ishihara error scores in deutan participants and reduced D-15 confusion index in protans. Despite the statistical significance in these changes, they were not substantial enough to constitute any diagnostic changes in individuals and the authors conclude that use of EnChroma is unlikely to affect career opportunities or daily living.

## 3.2. Modelling

### 3.2.1. Quantifying discriminability

To quantify the optimal change in discriminability with and without the EnChroma filter for an ideal observer who optimally exploits the available information, we considered the change in the gamut produced by a subset (1269) of surface reflectances for the patches in the matte-finish Munsell Book of Color taken from <https://www.uef.fi/web/spectral/munsell-colors-matt-spectrofotometer-measured>, reduced to the wavelength range 400 nm to 700 nm. We did this for each observer type separately in their optimal color space. We were interested in whether the size of the gamut increases, allowing for greater discriminability as the points will be more spread out. We quantified the spread as the standard deviation of the points (the Munsell colors) in optimal color

space along each axis. Table 8 gives the values for each observer type and each axis both with and without the glasses.

**Table 8. Spread of colors in optimal color space with and without glasses. Where we used labels L and M in the table to refer to different channels, recall that this will be different for different observer types e.g., S-(L + M) would be S-(L-L') for the Da observer**

Observer	Baseline standard deviation			Standard deviation with EnChroma		
	<i>Lum</i>	<i>S-(L + M)</i>	<i>L-M</i>	<i>Lum</i>	<i>S-(L + M)</i>	<i>L-M</i>
N	0.30	0.10	0.02	0.30	0.11	0.02
Da	0.30	0.11	0.004	0.30	0.11	0.01
Pa	0.30	0.10	0.01	0.30	0.11	0.01
D	0.24	0.09	N/A	0.24	0.10	N/A
P	0.24	0.08	N/A	0.24	0.10	N/A

The change in the spread of the points when the glasses are added is small for all axes of optimal color space in each observer type (see Table 8). Since the numbers are very small before the addition of the glasses, a better way to express the change in the size of the gamut (or change in discriminability) is to calculate the ratio of the standard deviations for each axis. If we divide the standard deviations with the glasses by the standard deviations without the glasses, a number greater than 1 implies an increase in discriminability along that axis and a number less than 1 implies a decrease. These ratios are shown in Table 9. The ratios suggest that discrimination along chromatic axes could be improved for all observer types, if they were to optimally exploit available information.

**Table 9. Change in spread of colors when glasses are added. As above, where we use labels L and M in the table to refer to different channels, recall that this will be different for different observer types e.g., S-(L + M) would be S-(L-L') for the Da observer**

Observer	Ratio		
	<i>Lum</i>	<i>S-(L + M)</i>	<i>L-M</i>
N	1.00	1.08	1.25
Da	0.99	1.05	1.37
Pa	1.00	1.12	1.08
D	0.99	1.05	N/A
P	0.99	1.15	N/A

### 3.2.2. Output of the ideal observer models

Figure 4 plots the FM100 Hue caps in optimal color space, both with (red circles) and without (black squares) the glasses, for each observer type. The plots show that the shape of the hue circle formed by the FM100 Hue caps in the optimal color space for trichromats is preserved in the optimal color spaces of anomalous trichromats. In dichromats this is not the case, as there is only a single axis of chromatic discrimination. However, these plots show how luminance can provide an extra cue to color in these observer types as the caps are not designed to be equiluminant for dichromat observers.

Table 10 compares the TES predicted by the ideal observer model for each observer type (see Ideal Observer Models) to our mean behavioral results. Broadly, the model captures these empirical results. For example, behaviorally, the ordering of the mean TES at baseline from best to worst was normal trichromat > protanomalous > protanope > deuteranomalous > deuteranope. A similar pattern can be seen in the model, where the ordering at baseline is normal trichromat >

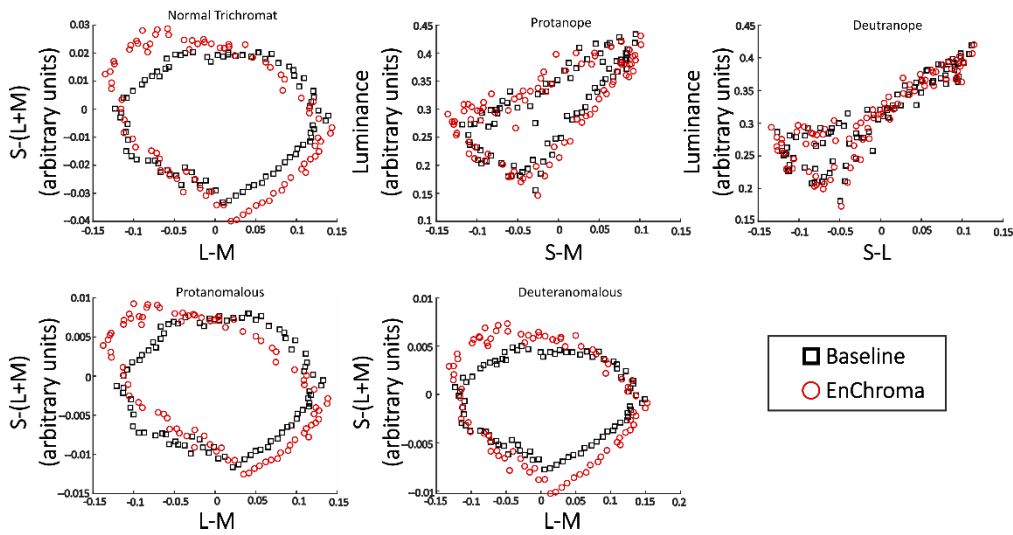


**Fig. 4.** Plots of the FM100 Hue caps in optimal color space for each observer type.

protanomalous > deuteranomalous > protanope > deuteranope. The order of protanopes and deuteranomalous is switched in the model but these two observer types showed very similar behavior empirically at baseline. Similarly, the model captures the pattern in TES behavior when the EnChroma glasses were worn. It does not capture the pattern across observer types in CA behavior equally well but does capture the direction of change in the CA angle for each observer type as they go from Baseline to using the EnChroma glasses (Table 11).

**Table 10. Total error scores produced by the ideal observer with and without the glasses alongside the behavioral data (reproduced from Table 4)**

	TES				
	Model	Baseline		EnChroma	
		Behavioral (M±SD)	Model	Behavioral (M±SD)	
Trichromat	40	46.50±27.25	72	72.67±28.81	
Protanope	164	202.40±65.39	168	221.40±76.48	
Deuteranope	184	256.00±64.78	168	249.33±63.25	
Protanomalous	52	174.00±71.48	80	184.33±75.02	
Deuteranomalous	68	204.80±85.56	88	186.80±91.21	

Most importantly, while the TES and CAs predicted by the ideal observer models may not perfectly match the behavioral data, they do tell the same overall story - that the EnChroma glasses may be more of a hindrance than a help in terms of TES, even when the available information is optimally exploited, and that they improve discrimination in some areas of the hue circle while worsening discrimination in others.

3.2.3. Modelling summary

As others have done previously [8,10,13,25] we modelled changes in the chromaticities of colored samples when viewed with and without the filtering lens and used this to make a prediction about the effect that these chromaticity changes have on discriminability of the colored samples. Moreland et al. [8,10] offer a similar prediction. Our prediction is different in that we quantify



**Table 11. Confusion angles produced by the ideal observer with and without the glasses alongside the behavioral data (reproduced from Table 5)**

	Confusion Angle			
	Baseline		EnChroma	
	Model	Behavioral (M±SD)	Model	Behavioral (M±SD)
Trichromat	-10.42	-22.05±49.69	25.57	1.06±47.74
Protanope	9.06	-0.38±8.18	30.86	13.12±23.77
Deuteranope	-10.66	-22.09±5.98	12.05	1.10±10.27
Protanomalous	-4.14	1.83±33.00	25.50	13.09±25.77
Deuteranomalous	-9.24	-10.55±30.68	13.63	-7.35±31.74

discriminability in optimal color spaces, unique for each observer type (N, D, P, Da, Pa), that optimally represent the variation in the cone excitations (analogous to processing in the ganglion cell layer and the LGN) after von Kries adaptation (allowing for color constancy). These properties of our ideal observer are motivated by previous work suggesting that changes in post-receptoral gain optimize post-receptoral processing of color signals in anomalous trichromats [26], maintaining a trichromatic color space in anomalous trichromacy, but one whose dimensions differ to that of normal trichromats [27]. In addition, we developed ideal observer models of the FM100 Hue test for each observer type within these optimal color spaces. The ratios in Table 9 suggest that discrimination along chromatic axes could be improved for all observer types, however these do not translate to an improvement on the FM100 Hue test. Overall, our findings support previous literature showing that the EnChroma glasses will not aid CVDs in passing a standard test of color blindness (the FM100 Hue test; [28]).

#### 3.2.4. Modelling limitations

We would like to make the reader aware that our modelling approach has its limitations. First, as we have stressed, we aimed to create an ideal observer model by first defining optimal color spaces for each of our observer types. To define the optimal color spaces, we assumed that post-receptoral color channels could optimally represent the available information at the retina by adapting the weight placed on the input from each cone type. Secondly, we assumed perfect von Kries scaling of the incoming retinal signals, allowing for perfect adaptation to the EnChroma lenses. Even if such perfect adaptation was possible, it is not clear that it would be possible after only wearing the lenses for 30 minutes, as in our behavioral experiment. Moreover, to derive the optimal color spaces, we chose to use a set of measured Munsell surface reflectances. We chose this set of surfaces as they are closely related to the colors of the caps used in the FM100 Hue test. However, this set of surfaces is not representative of the natural set of surface reflectances experienced in daily life so training our model to optimally represent differences among Munsell surfaces may not be representative of the set of surfaces that the visual system learns to differentiate. However, despite its limitations, we still believe that the modelling offers further insight than could be gained from our behavioral data alone, as it demonstrates that even when the changed (when wearing the EnChroma lenses) signals available at retina are optimally exploited in this way, this does not lead to a predicted improvement in FM100 Hue error scores.

## 4. Conclusions

The aim of this study was to investigate the efficacy of EnChroma glasses to enhance the chromatic discrimination abilities of individuals with known color-vision phenotypes. Using a large, well-categorized sample of participants, our study is in line with the reports of Gómez-Robledo et al [12] as we found little evidence for an overall improvement in chromatic discrimination for any

CVD subtype and confirm that EnChroma filters cannot be used to pass diagnostic tests. Given the individual differences in cone spectral sensitivities between observers of all subtypes, a “one size fits all” notch-filter solution is not going to work for every color-deficient individual and explains, to some extent, the variability in the data. EnChroma’s sales pitch that the notch filter is placed at the “precise point where this confusion or excessive overlap of color sensitivity occurs” [4] is therefore misleading.

The filters cannot undo an existing color deficiency, but they might boost signals in a subset of anomalous trichromats. The findings of Werner et al. [16] and Rabin et al. [18] provide evidence for such a potential compensatory effect of EnChroma filters to enable some anomalous trichromats to distinguish between red-green shades previously not perceived at a conscious level. So, there is no doubt that some enhancement does take place of the incoming signals and it is possible that, once these signals have passed the threshold to conscious awareness, they are being attended to, at a higher level of cortical processing where signals could be amplified or perceptual learning can take place [26,29]. An excellent review of compensatory adjustments to somewhat compromised color-anomalous visual systems has been provided by Isherwood et al. [30]

Nevertheless, if we accept the potentially enhancing effect of EnChroma filters to improve the experience of some colors in the environment in some individuals, it must be remembered that it will be at the expense of color discrimination elsewhere in their color space. At least for the moment, the possibility of altered color vision allowing for the experience of normal color vision remains to be solved in the future [31].

**Acknowledgements.** We would like to thank our many participants for giving up their time and supporting our study.

**Disclosures.** The authors declare that there are no conflicts of interest related to this article.

**Data availability.** Data underlying the results presented in this paper are available in Ref. [32].

**Supplemental document.** See [Supplement 1](#) for supporting content.

## References

1. B. C. Regan, J. P. Reffin, and J. D. Mollon, “Luminance noise and the rapid determination of discrimination ellipses in colour deficiency,” *Vision Res.* **34**(10), 1279–1299 (1994).
2. J. Neitz and M. Neitz, “The genetics of normal and defective color vision,” *Vision Res.* **51**(7), 633–651 (2011).
3. B. L. Cole, “The handicap of abnormal colour vision,” *Clin. Exp. Optometry* **87**(4-5), 258–275 (2004).
4. EnChroma, “How EnChroma Glasses Work,” <https://enchroma.co.uk/pages/how-enchroma-glasses-work>.
5. A. Seebeck, “Ueber den bei manchen Personen vorkommenden Mangel an Farbensinn,” *Ann. Phys. Chem.* **118**(10), 177–233 (1837).
6. L. T. Sharpe and H. Jägle, “I used to be color blind,” *Color Res. Appl.* **26**(S1), S269–S272 (2001).
7. A. E. Salih, M. Elsherif, M. Ali, N. Vahdati, A. K. Yetisen, and H. Butt, “Ophthalmic Wearable Devices for Color Blindness Management,” *Adv. Mater. Technol.* **5**(8), 1901134 (2020).
8. J. D. Moreland, S. Westland, V. Cheung, and S. J. Dain, “Quantitative assessment of commercial filter “aids” for red-green colour defectives,” *Ophthalmic and Physiological Opt.* **30**(5), 685–692 (2010).
9. Comité Européen de Normalisation (CEN), *Personal Eye-Equipment – Sunglasses and Sunglare Filters for General Use and Filters for Direct Observation of the Sun.* (2007).
10. J. Moreland, V. Cheung, and S. Westland, “Evaluation of a model to predict anomalous-observer performance with the 100-hue test,” *J. Opt. Soc. Am. A* **31**(4), A125–A130 (2014).
11. R. Mastey, E. J. Patterson, P. Summerfelt, J. Luther, J. Neitz, M. Neitz, and J. Carroll, “Effect of “color-correcting glasses” on chromatic discrimination in subjects with congenital color vision deficiency,” *ARVO Annual Meeting* **57**(12), 192 (2016).
12. N. Almutairi, J. Kundart, N. Muthuramalingam, J. Hayes, and K. Citek, “Assessment of Enchroma Filter for Correcting Color Vision Deficiency,” (Pacific University (Oregon), 2017).
13. L. Gómez-Robledo, E. M. Valero, R. Huertas, M. A. Martínez-Domingo, and J. Hernández-Andrés, “Do EnChroma glasses improve color vision for colorblind subjects?” *Opt. Express* **26**(22), 28693 (2018).
14. K. Bastien, D. Mallet, and D. Saint-Amour, “Characterizing the Effects of Enchroma Glasses on Color Discrimination,” *Optom Vis Sci* **97**(10), 903–910 (2020).
15. V. N. V. Varikuti, C. Zhang, B. Clair, and A. L. Reynolds, “Effect of EnChroma glasses on color vision screening using Ishihara and Farnsworth D-15 color vision tests,” *J. AAPOS* **24**(3), 157.e1 (2020).
16. J. S. Werner, B. Marsh-Armstrong, and K. Knoblauch, “Adaptive Changes in Color Vision from Long-Term Filter Usage in Anomalous but Not Normal Trichromacy,” *Curr. Biol.* **30**(15), 3011–3015.e4 (2020).

17. A. M. Derrington, J. Krauskopf, and P. Lennie, "Chromatic mechanisms in lateral geniculate nucleus of macaque," *The J. Physiol.* **357**(1), 241–265 (1984).
18. J. Rabin, F. Silva, N. Trevino, H. Gillentine, L. Li, L. Inclan, G. Anderson, E. Lee, and H. Vo, "Performance enhancement in color deficiency with color-correcting lenses," *Eye* **36**(7), 1502–1503 (2022).
19. H. le Sueur, J. D. Mollon, J. Granzier, and G. Jordan, "Counterphase modulation photometry: comparison of two instruments," *J. Opt. Soc. Am. A* **31**(4), A34 (2014).
20. A. J. Vingrys and P. E. King-Smith, "A quantitative scoring technique for panel tests of color vision," *Investigative Ophthalmology and Visual Science* **29**(1), 50–63 (1988).
21. D. L. Ruderman, T. W. Cronin, and C.-C. Chiao, "Statistics of cone responses to natural images: implications for visual coding," *J. Opt. Soc. Am. A* **15**(8), 2036 (1998).
22. J. von Kries, "Beitrag zur Physiologie der Gesichtsempfindung," *Arch. Anat. Physiol* **2**, 505–524 (1878).
23. J. Krauskopf, D. R. Williams, and D. W. Heeley, "Cardinal directions of color space," *Vision Res.* **22**(9), 1123–1131 (1982).
24. P. DeMarco, J. Pokorny, and V. C. Smith, "Full-spectrum cone sensitivity functions for X-chromosome-linked anomalous trichromats," *J. Opt. Soc. Am. A* **9**(9), 1465 (1992).
25. J. M. M. Linhares, P. D. Pinto, and S. M. C. Nascimento, "The number of discernible colors perceived by dichromats in natural scenes and the effects of colored lenses," *Visual Neuroscience* **25**(3), 493–499 (2008).
26. A. E. Boehm, D. I. A. MacLeod, and J. M. Bosten, "Compensation for red-green contrast loss in anomalous trichromats," *Journal of Vision* **14**(13), 19 (2014).
27. J. M. Bosten, J. D. Robinson, G. Jordan, and J. D. Mollon, "Multidimensional scaling reveals a color dimension unique to 'color-deficient' observers," *Curr. Biol.* **15**(23), R950–R952 (2005).
28. M. Á. Martínez-Domingo, E. M. Valero, L. Gómez-Robledo, R. Huertas, and J. Hernández-Andrés, "Spectral filter selection for increasing chromatic diversity in CVD subjects," *Sensors* **20**(7), 2023 (2020).
29. K. E. M. Tregillus, Z. J. Isherwood, J. E. Vanston, S. A. Engel, D. I. A. MacLeod, I. Kuriki, and M. A. Webster, "Color Compensation in Anomalous Trichromats Assessed with fMRI," *Curr. Biol.* **31**(5), 936–942.e4 (2021).
30. Z. J. Isherwood, D. S. Joyce, M. K. Parthasarathy, and M. A. Webster, "Plasticity in perception: insights from color vision deficiencies," *Fac. Rev.* **9**, 8 (2020).
31. K. Mancuso, M. Neitz, W. W. Hauswirth, Q. Li, T. B. Connor, J. A. Kuchenbecker, M. C. Mauck, and J. Neitz, "Long-Term Results of Gene Therapy for Red-Green Color Blindness in Monkeys," *Invest. Ophthalmol. Visual Sci.* **51**(13), 6292 (2010).
32. S. Aston, "The effects of commercial notch-filters on the chromatic discrimination abilities of colour vision deficient observers," (2021).